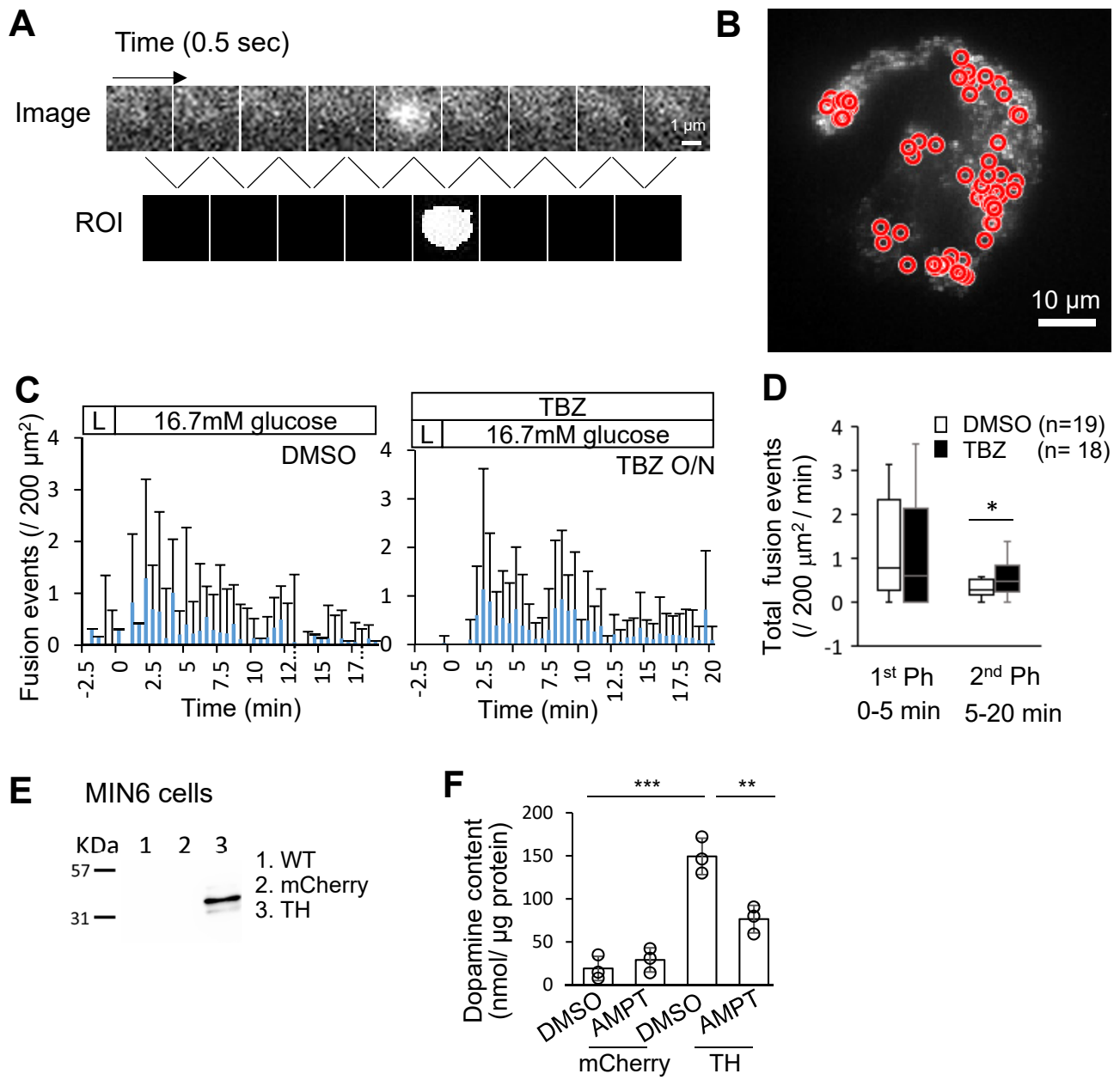


SUPPLEMENTARY DATA

Dopamine negatively regulates insulin secretion
through activation of D1-D2 receptor heteromer

Fumiya Uefune, Toru Aonishi, Tetsuya Kitaguchi, Harumi Takahashi,
Susumu Seino, Daisuke Sakano, Shoen Kume

Supplementary Figure S1



Supplementary Figure S1. Automatic detection of fusion events using Matlab and analysis of the inhibition by TBZ on insulin granule exocytosis.

(A, B) Automatic detection of fusion events using Matlab. (A) Images were acquired every 0.5 sec. Fusion and release of insulin granules are detected by increased intensity and diffusion of Venus protein (Upper). Differences in intensities of two consequent frames (ΔX) were calculated with the equation shown below. ROIs were identified by filtering the intensity differences. Then the ROIs were subtracted with the thresholds of areas (lower).

X = Intensity of pixel. $\Delta X = X(t+1) - X(t)$

If $\Delta X > X$ Threshold $\Delta X = 1$, else $\Delta X = 0$

ROI; $S(\Delta X = 1) > S$ threshold (S : Area)

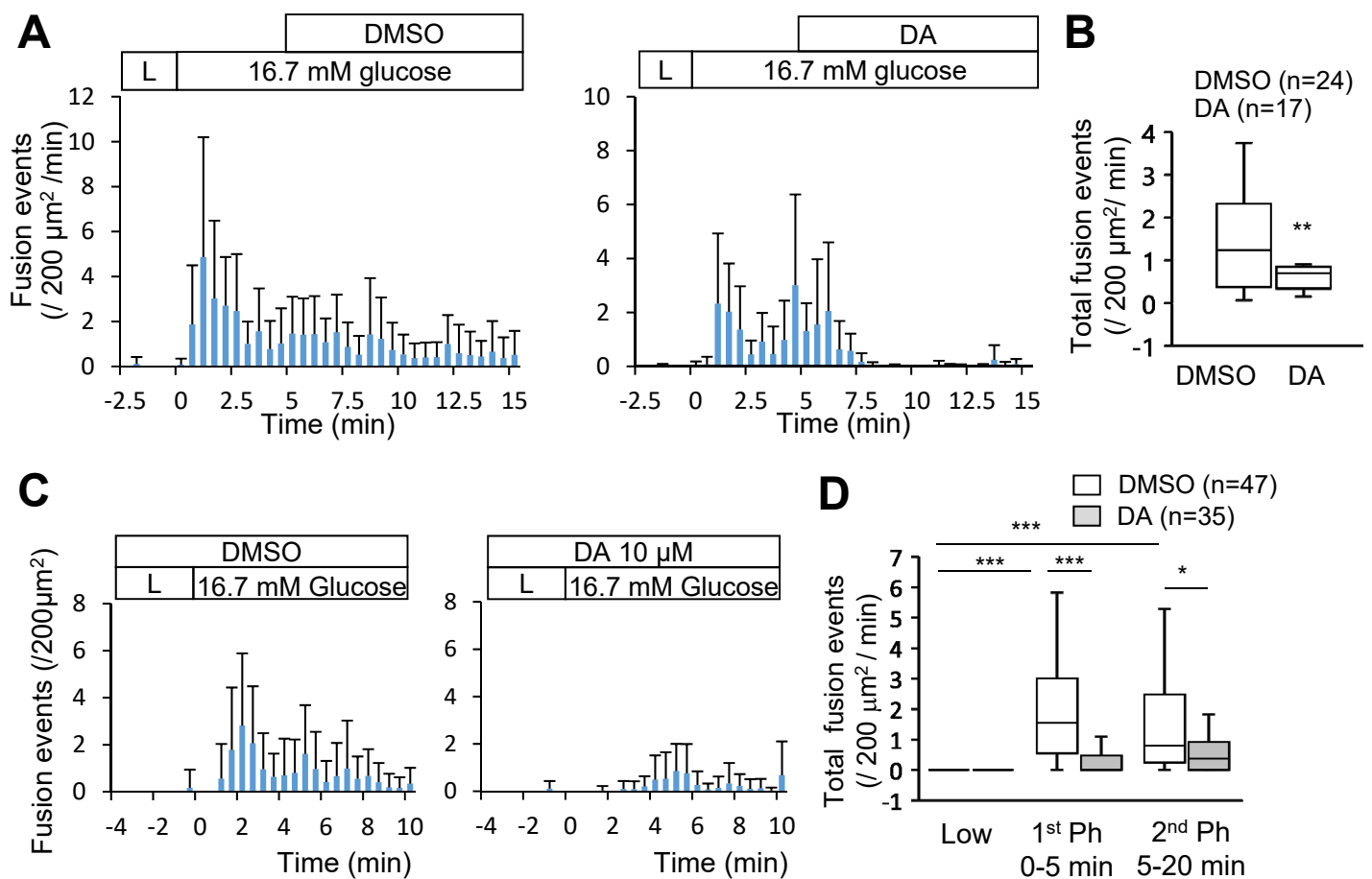
Image sequences: $2.99 \mu\text{m} \times 2.99 \mu\text{m}$, 23×23 pixels, Scale bars: $1 \mu\text{m}$.

(B) Red circles mark the positions of fusion events that occurred. Scale bars: $10 \mu\text{m}$.

(C, D) Inhibition by $10 \mu\text{M}$ TBZ on insulin granule exocytosis. (C) Histograms of fusion events (per $200 \mu\text{m}^2$) at 30-sec intervals in pancreatic beta-cells challenged with 16.7 mM glucose in the presence or absence of TBZ. (D) The average number of fusion events ($/200 \mu\text{m}^2 / \text{minute}$) in the second phase (5–20 min) increased in TBZ (black bars)-treated beta-cells compared to the controls (DMSO; white bars).

(E, F) Overexpression of TH in MIN6 cells. (E) Western blot analysis revealed increased TH protein level in TH but not control (WT) or mCherry overexpressed MIN6 cells.

(F) DA contents analyzed by ELISA. An increase in DA content in TH overexpressing MIN6 cells, which was reversed by $10 \mu\text{M}$ AMPT treatment, was observed. Values represent the mean \pm SD (C, F), or medians in box and whisker plots (D). Representative underlying imaging data for (C) are available online (DOI:10.6084/m9.figshare.17048318).

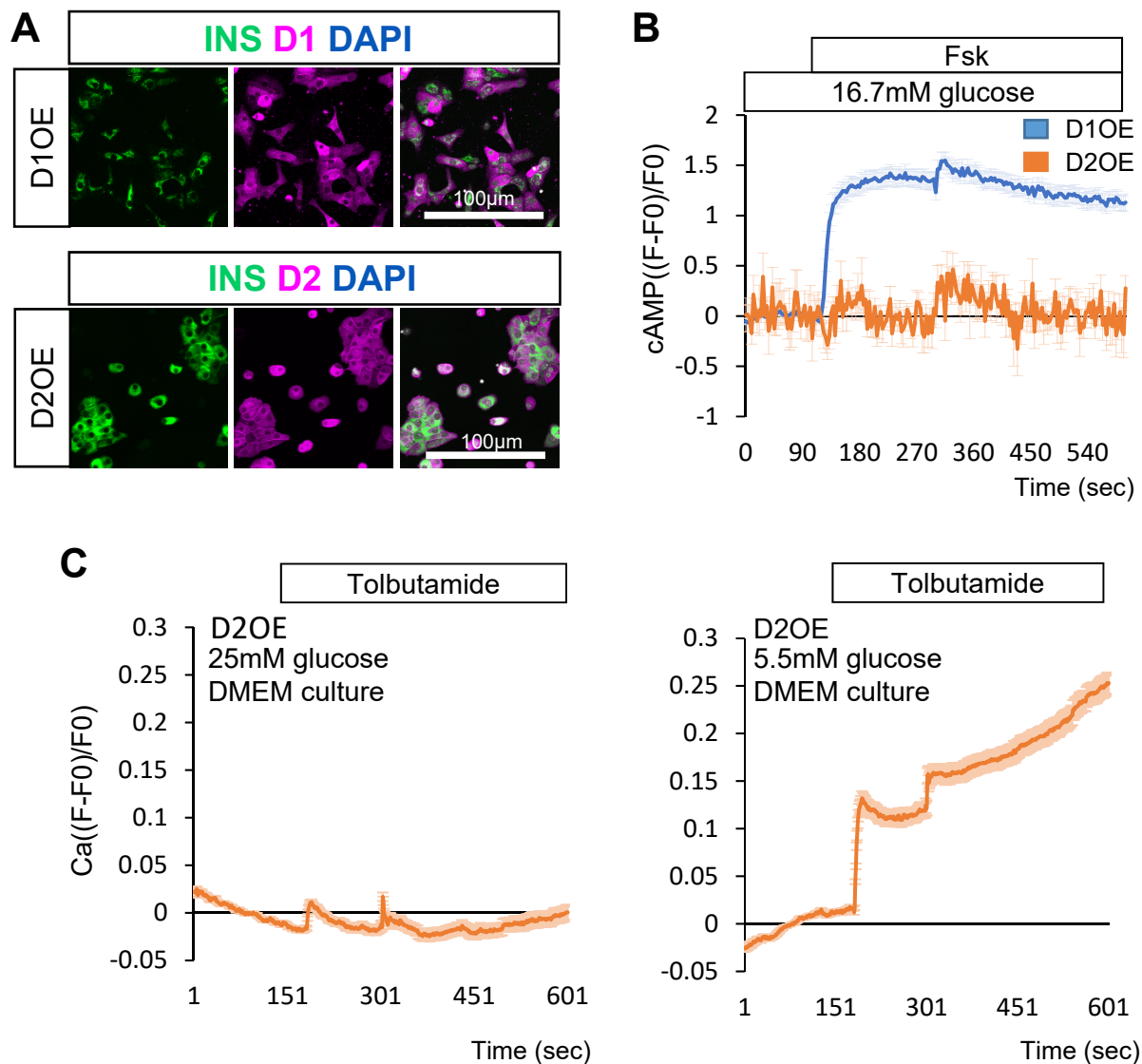


Supplementary Figure S2 Exogenous addition of DA exerted negative effects on glucose-induced insulin granule exocytosis.

(A, B) The addition of 10 μM DA to the second phase of insulin exocytosis decreased fusion events, as revealed by TIRFM. Histograms of fusion events per $200 \mu\text{m}^2$ at 30-sec intervals in pancreatic beta-cells stimulated by 16.7 mM glucose \pm DA. (B) The average number of fusion events ($/200 \mu\text{m}^2/\text{minute}$) for 15 minutes after DA addition.

(C, D) Before the high glucose challenge, the exogenous addition of DA decreased the first and second phases of insulin exocytosis fusion events. (C) Histograms of fusion events per $200 \mu\text{m}^2$ at 30-sec intervals in pancreatic beta-cells stimulated by 16.7 mM glucose \pm DA. (D) The average number of fusion events ($/200 \mu\text{m}^2/\text{minute}$) in the first (0–5 min) and second phases (5–20 min). Values represent the mean \pm SD (A, C), medians in a box and whisker plot (B, D). Statistical analysis by Student's *t*-test (B) or one-way ANOVA and Dunnett multiple comparisons tests (D).

Representative underlying imaging data are available online (DOI:10.6084/m9.figshare.17048318).



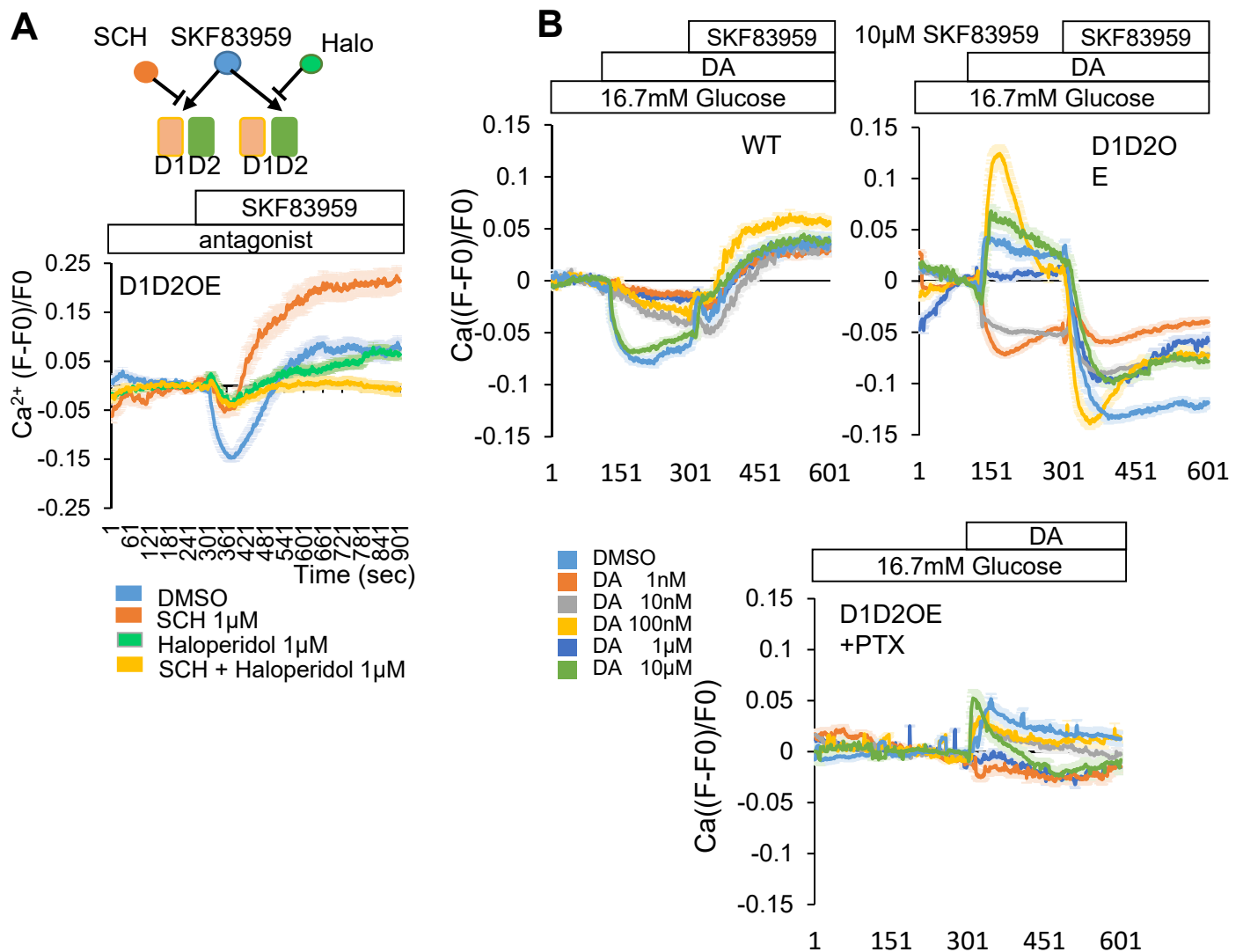
Supplementary Figure S3. Immunochemical analysis of pancreatic beta-cells overexpressing D1 or D2 receptor.

(A) Primary beta-cells infected with adenovirus bearing D1 (upper) or D2 (lower) receptor cDNA was detected for INS (green), D1 (upper), or D2 (lower) receptor (red) and counterstained with DAPI (blue). Identical images in Fig. 4A and B, with lower contrasts.

(B) D1OE or D2OE beta-cells were challenged with Frk (10 μM) at high glucose. Frk triggered an increase in cAMP in D1OE but not in D2OE beta-cells.

(C) D2OE beta-cells cultured at high (25 mM; left) for 2 overnights or switched to low (5.5 mM; right) glucose for the last overnight incubation were challenged with tolbutamide (100 μM). Tolbutamide triggered an increase in Ca²⁺ flux in beta-cells cultured at low but not high glucose.

Representative underlying imaging data for (B, C) are available online (DOI:10.6084/m9.figshare.17048318).

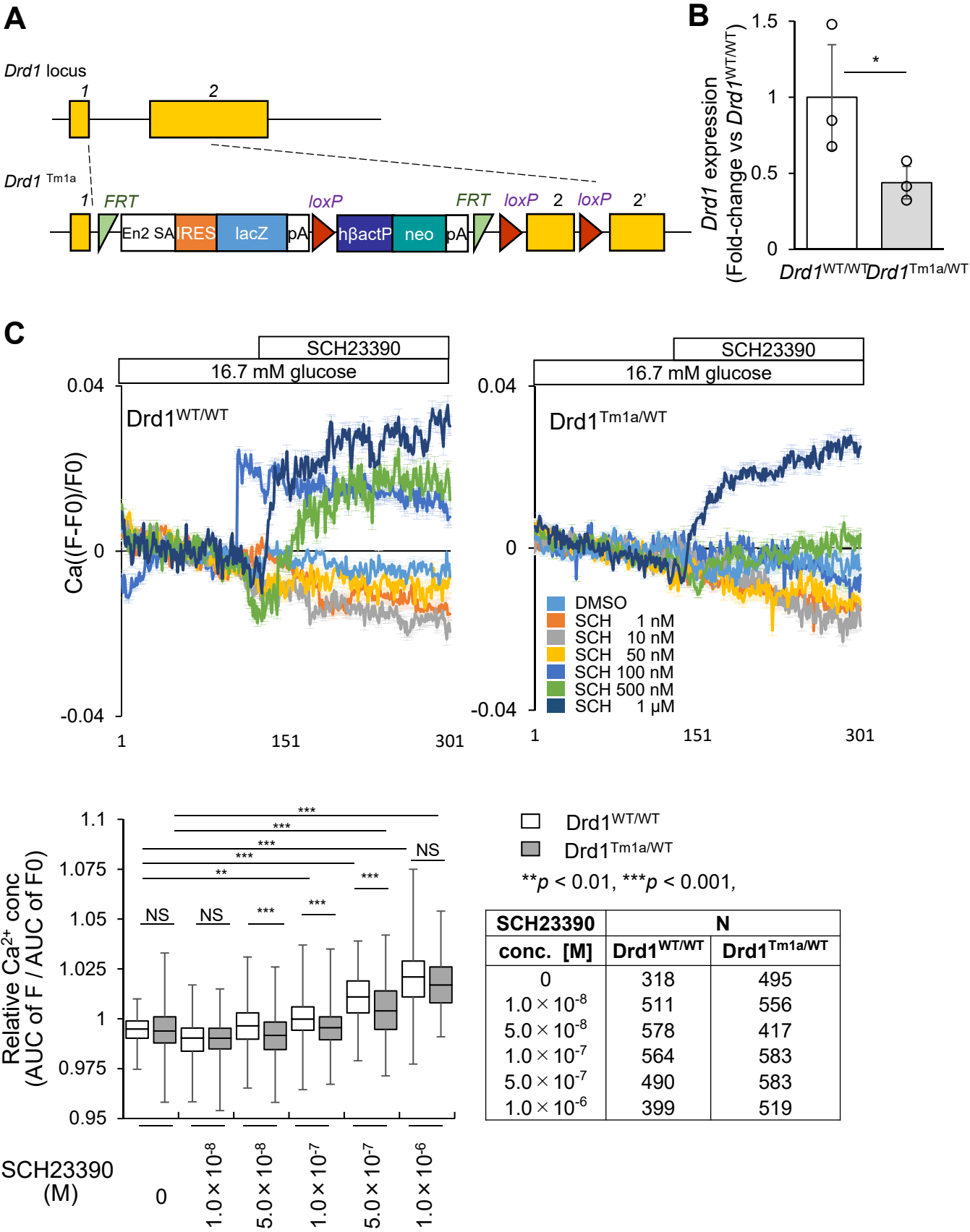


Supplementary Figure S4. D1 and D2 antagonists compete with SKF83959 for binding to the D1-D2 heteromer.

(A) (Upper) SKF83959 binds to both the D1 and D2 receptor sites in the D1-D2 heteromer. D1 and D2 antagonists compete with SKF83959 for their binding to the D1-D2 heteromer. (lower) Intracellular Ca²⁺ dynamics are visualized using Fluo-4-AM. Images were acquired every sec. The inhibition of glucose-stimulated Ca²⁺ flux in D1D2OE beta-cells by 10 μM SKF83959 was rescued by adding D1 antagonist SCH23390 or D2 antagonist haloperidol or both (each at 1 μM). Values represent the mean ± SD.

(B) Control WT (left) or D1D2OE (upper right, lower) beta-cells were challenged with high glucose (16.7mM) in the presence of various concentrations of DA, in the absence (upper panels) or presence (lower) of PTX (100 ng/ml), and tested for the effects of SKF83959 (10 μM, upper panels). Intracellular Ca²⁺ dynamics are visualized using Fluo-4-AM. Images were acquired every sec. SKF83959 showed a transient inhibitory effect on Ca²⁺ flux. Representative underlying imaging data for (A, B) are available online (DOI:10.6084/m9.figshare.17048318).

Supplementary Figure S5



Supplementary Figure S5 D1 antagonist SCH23390 to increase glucose-stimulated Ca²⁺ flux is partially inhibited in heterozygous D1 receptor knockout (*Drdl*^{tm1a/WT}) islets.

(A) The D1 receptor knockout (*Drdl*^{tm1a/WT}) mouse generation. The schematic drawing of the ES cell line for generating the *Drdl*^{tm1a/WT} mutant.

(B) *Drdl* expression level in the heterozygous mutant *Drdl*^{tm1a/WT} is about half of the control WT mice (*Drdl*^{WT/WT}), confirming that the *Drdl* gene was successfully knocked-out. Means±SD is shown (n=3). Significant differences are shown as **p* < 0.05, by student *t*-test.

(C) Islets from the WT littermates (*Drdl*^{WT/WT}, upper left) or *Drdl*^{tm1a/wt} (upper right) were visualized for Ca²⁺ dynamics using Fluo-4-AM. D1 antagonist SCH23390 to increase glucose-stimulated Ca²⁺ flux was significantly smaller in the heterozygous *Drdl* mutant at 50 nM, 100 nM, and 500 nM than in the WT (lower panel). Significance are shown as ***p* < 0.01, ****p* < 0.001, one-way ANOVA and Dunnett multiple comparisons test. Representative underlying imaging data for (C) are available online (DOI:10.6084/m9.figshare.17048318).